Department of Neuroscience, Psychology and Behaviour

Infraslow dynamics across cortical layers

Research Project

Geofrey Oteng Phutietsile

(SN 199043602)

Supervisor: Dr. Michael Okun

Introduction

One of the most important open questions in neuroscience is how neurons code information into spike trains. The basic and frequently considered concept is rate coding [1]. It assumes that the information is coded by the spike rate, which is mostly calculated as a spike count average. The spike rate, however, does not take into consideration how the spike times are distributed in the given timeline, different spike sequences can yield the same spike rate. So there is the possibility that there is more information in a spike train than what can be coded using the spike rate. A natural extension of the rate coding, which better reflects the specific spike timing, is variability coding [2], sometimes referred to as "spike-time code"[4]. In such a case, it is assumed that the variability in spike trains also carries information. The significance of such a coding system that uses the permutation of spike-times is that it would confer a higher communication bandwidth compared to the simple rate code. But whether the variability does indeed encode additional information or is just noise or uncharacterized components of an actual signal is still a topic of debate. This has not been determined outright i.e whether the irregularity of spike distribution is a feature of the spiking neuron or a "bug."

Many studies have however shown that spike generation is a fairly reliable and deterministic process; with studies by Mainen and Sejnowski (1995) demonstrating spiketrains that where reproducible to less than 1 msec when neurons from slices of the rat cortex where injected with complex time-varying currents. Such observations have led to the idea that neural spiking variability may be a product of unreliable synapses [10] that contribute to the irregularity seen in a neurons spiketrains.

At any rate, this is one of the reasons why studies that look into measures of neuron spiking variability are of importance, given that the existence of spiking irregularity exists at the individual level of the neuron. The aim of such efforts would be to quantify this variability. One of the most widely used measures of variability of spike trains is calculation of the Fano factor (ff). For a given time window (bin), the Fano factor is given by the ratio of a neuron's observed spike-count variance to its spike-count mean. The precision of this estimator has been found to strongly depend on the length of the (sampling) window/binsize[3]. If the probability distribution of spiking could be modelled by a theoretical Poisson then the FF of neurons be at or near unity.

The refractoriness of neurons means that neural spiking is not a purely Poisson process because the advent of one spike is to an extent dependent on the timing of the previous spike. The refractoriness thus reduces the randomness in spiking, increasing regularity in spiking and therefore reducing the variance in spike counts registered from one bin to the next. This means that any finite refractory period reduces the Fano Factor from Poisson 1 to below 1, as the fraction of variance to mean decreases.

In a previous experiment by M. Okun et tal (2019)[12], the experimenters found that they could closely model Fano factors and Firing rates by taking into account information regarding the power density spectrum (PSD) and the Interspike Intervals (ISI's) of the neuron. In this experiment, we attempt to characterize another possible predictor of what the FF value a neurons is likely to have. This is the depth that a neurons that a neuron inhabits along the cortex; using the visual cortex of mice for the experiment.

Methodology

The spiking data used was collected by Senzai et tal [11] from 19 rodents. Extracellular potentials where captured with a single shank 64-site linear silicon probe with each rodent recording session lasting an average of 5.3 hours (2-9hrs). The probe was implanted into the visual cortex of the rodents to record activity of neurons during free behaviour of the rodents in their cage habitats (fig 1).

Figure 1

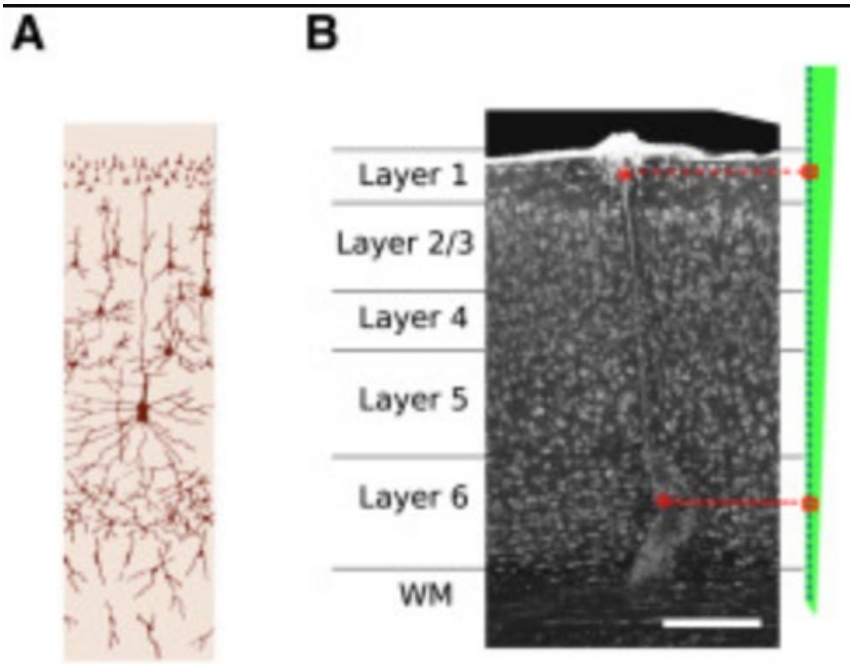

(A) Schematic of the spatial arrangement of the main cellular types in V1.
(B) Histological verification of probe location along V1 cellular layers. Small electrolytical lesions were performed with the two electrodes highlighted on the silicon probe sketch (red rectangles)

Source [11]

Description of the dataset

The data used to make the analysis came from three main datatypes; 1) *.res 2)*.clu and 3)* meanWaveforms. The *.res file contained all the times at which the spikes where recorded whilst the corresponding *.clu file contained the cluster identity of the putative neural cluster that elicited the spikes. Matlab code was designed to use the two datatypes to sort all the spiketimes to their putative neural clusters; giving rise to 1472 distinct spiketrains .

Identifying the Cortical Layer Position of Each Neural Cluster

The position of the individual 64 channels of the recording shank was worked out in the original experiment by Senzai et tal (2019) such that the task at hand was to workout the position of the clusters with respect to the recording probe's 64 recording channels. Code was designed that

identified the cluster that records the strongest spiking signal, in the form of fluctuating extracellular potential. To do this; the mean-Waveforms datatype was used. For each neural cluster, the extracellular potential differences recorded by each of the 64 channels over a number of time points was scanned. The minimum and maximum potential difference recorded along each channel's time dimension was used to work out the peak to peak voltage/PD that each channel recorded for that singular clusters spiking activity. The channel that recorded the largest peak to peak voltage was then assigned to that neuron. This way, each of the 64 channels along the recording probe was assigned a collection of neurons that are most nearest to it relative to the other channels.

Computation Of The Firing Rates Of Identified Neural Clusters

With the spiketrains of each putative neuron computed and stored, the firing rate of each putative neuron was worked out as the quotient of the spike count of each spiketrain and the duration of recording. The spike-count would be the "size" of the spiketrain whilst the duration of a recording for one of the 19 rodents was simply taken as the last spiketime found in the corresponding *.res file..

Distribution of firing rates across the cortex

Once the cortical layer position of the neurons along the cortex has been worked out together with the firing rates, we will then analyse the firing rate distribution of the neurons across the cortical layers. For a single mouse, a suitable statistical measure will be used to workout if there is any correlation and or dependence of the firing rate on the cortical position that the neuron inhabits along the vertical axis. This will be extended to the other 18 mice and a suitable statistical measure will be employed to workout if any results obtained are of statistical significance.

Fano-Factor distribution

To work out the Fano factor, the variance in the spike-count produced by each neuron as well as the mean spike count have to be computed. The "trials" where generated by "binning" the spiketrains using particular binsizes.

Normally, the variance is to do with variation in spike count observed in a neurons response to presentation of the same stimuli. In this spike recording experiment however, stimulus presentation was not conducted. Instead, the variance measure that will be used will be one referring to spike count variance observed from one chosen time period to the next. For a 9 hour recording for example, choosing durations of 100 seconds will create "324" trials. Further, the 100 time period will be binned into an appropriate number of bins, like 20msec time bins within which the spike counts will be computed. This will create a distribution of spike counts whose variance can be calculated. The mean spike count, which is the spike count number most likely to be obtained can be worked out from the probability distribution. With both quantities obtained, the Fano factor quantity of each neuron can be worked out; as the ratio of the spike count variance to the mean spike count.

Once this is done, the fano factor of all the clusters across the vertical axis of the cortex will be known. This will allow us to use a suitable statistics measure to workout if there is any correlation between the FF and location of a neuron on the cortex laminar. The statistical significance of any

correlation found will be calculated using suitable statistical significance measure. The type of correlation/dependence, if any, will also be probed, for the nature of its linearity.

used to record which included identified cluster ID's together with their elicited spikes/spiketimes and mean waveforms. The data was then used to workout the spiketrains of 1472 putative neurons, followed by computation of their firing rates, FFs and location of neurons along axis of the visual cortex lamina

Results and Discussion

Consistent with findings from other publications where the logarithm of the firing rates was observed to be well fit with a Gaussian distribution[8], the firing rates of neurons in this analysis where also observed to be lognormally distributed amongst the neuronal population(fig.2).

Figure 2

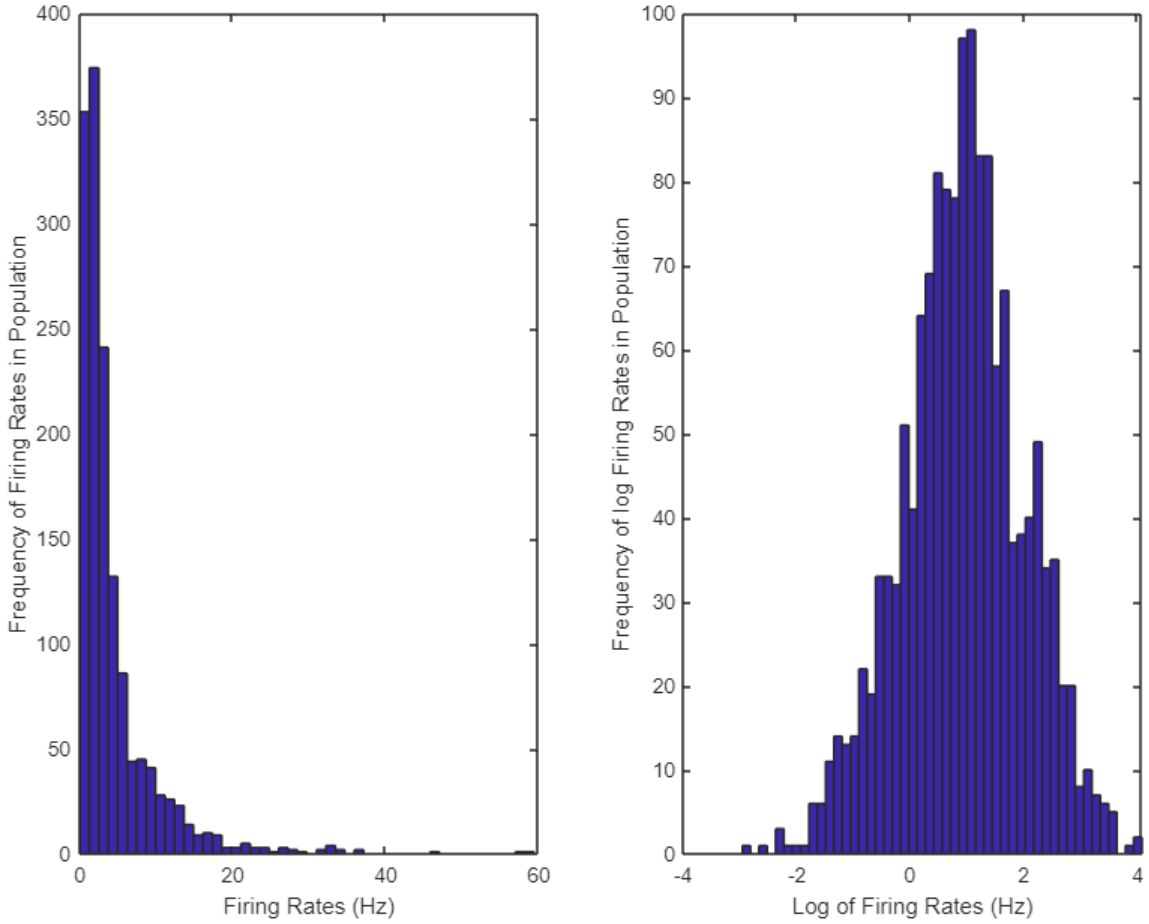

LEFT: Firing rates of neurons plotted in the linear scale
RIGHT: Skewed lognormal distribution of firing rates

Plots of the firing rates against the lamina position from all rodents (n=19) where carried out and superimposed (fig 3A); revealing that the firing rates of neurons increased with depth into the visual cortex as a general rule in all mice recorded(fig3A,B). An even stronger pattern is observed when averaging the firing rates of neurons at each channel.

Figure 3

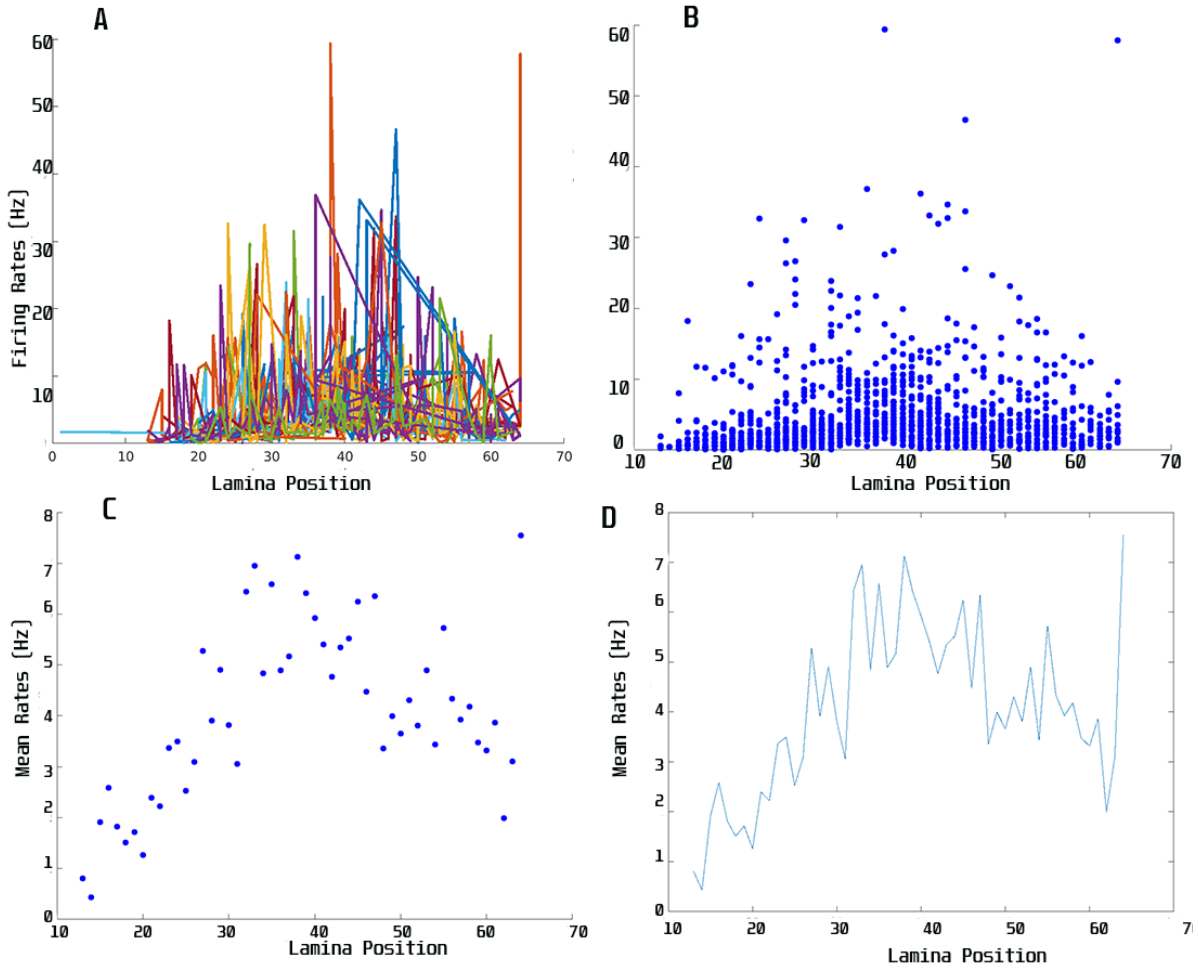

Panel A: Firing rates of all 1472 neurons plotted on a linear scale against lamina position (TOP), mean of firing rates averaged per channel against lamina position (BOTTOM)
Panel B: Firing rates of all neurons plotted on a log scale (TOP), mean of the logarithm of firing rates plotted against lamina position

Poisson spike trains (n=1472) where generated using the firing rates of corresponding real/putative neurons and plots of their firing rates where made. Because firing rates of the actual neurons were used in generating the Poisson trains, the plot of their rates where identical with figure 3. The difference between the Poisson spike trains that where artificially generated and the spiketrains from the actual neurons was the size of Fano factors measured, as will be described subsequently.

As the binsize tends to zero msec, the Fano factor of a spike train tends to unity:

$$\lim_{t\to 0} FF_t = \lim_{t\to O} \frac{Var(N_t)}{E(N_t)} = 1$$

This is because when the binsize becomes small enough to accommodate only one spike (action potential); which lasts about 1-2msec, then there can only be two outcomes, zero spike or 1 spike. Thus each time window has a Bernoulli event of zero or 1 spike.

For spiking rate "r" and time period "Δ", variance and mean of Bernoulli spiking event are as follows:

Variance=$r\Delta(1 - r\Delta)$

Mean= $r\Delta$

Thus the Fano factor as "Δ→ 0" is unity:

$$\lim_{\Delta \to O} \frac{r\Delta(1-r\Delta)}{r\Delta} = 1$$

Thus Fano factors of unity or close to unity are expected when small enough binsizes are used to segment the spike train. Such Fano factors would be invariant to changes in external factors because they exist by mathematical decree. And so unsurprisingly; neurons across all lamina positions have FFs close to unity when small enough binsizes are used. However as the size of the bin is progressively increased, the FFs not only increase in magnitude overall, but they increase the deeper into the cortex the neurons are being recorded from (fig 4); peaking around channel 55 before decreasing again(fig). The increase in Fano factors with increase in choice of binsize used is by mathematical decree because by doubling the binsize each time to produce the 17 different binsizes used in this experiment; we reduce the number of bins in the spike-train overall and scale up the mean spike count. The scaled up mean value is then squared and multiplied in the process of computing the variance; causing the variance to mean ratio to increase at a given constant linear rate. Thus for channels 29 and 55 as two examples, the relationship between the increase in mean FFs and increase in binsize is characterized by a straight line(fig 5) (R-squared>0.98), suggesting that each of the 17 FFs obtained are consistent with a single FF for that particular channel, that is simply being scaled up or down by a constant factor[13].

Figure 4

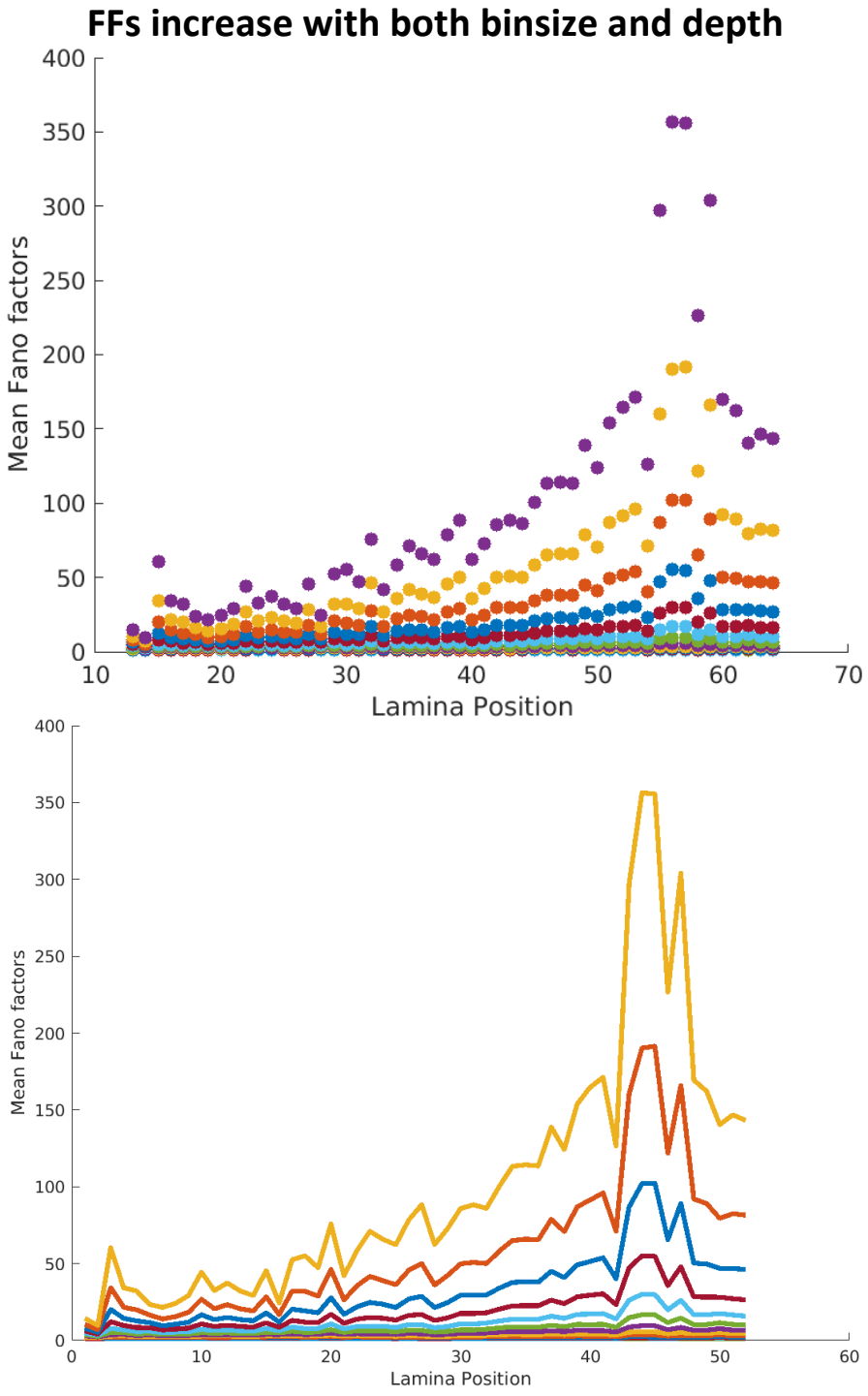
FFs increase with both binsize and depth
Mean Fano factors
Lamina Position
Mean Fano factors
Lamina Position

Figure 5

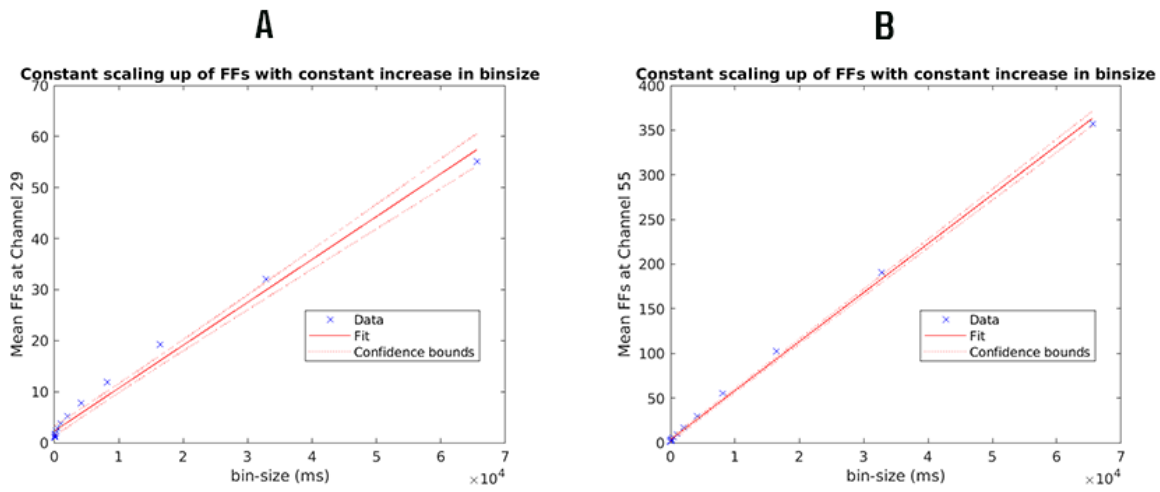

As was described previously. The Fano factors values are able to distinguish between real and Poisson neurons of the same. The Poisson spiketrains where invariant with changes in choice on binsize and depth into the cortex, remaining near or at unity the entire time(fig 6). This parallels findings by Okun et tal (2019) where instead of Poisson spiketrains, used ISI-shuffled spiketrains that where shown to have near unity FFs that where invariant with increase in binsize whilst the real neurons had fano factors that where several folds.

Figure 6

Poisson FFs Remain At Or Near Unity And Invariant To Changes in Binsize and Depth

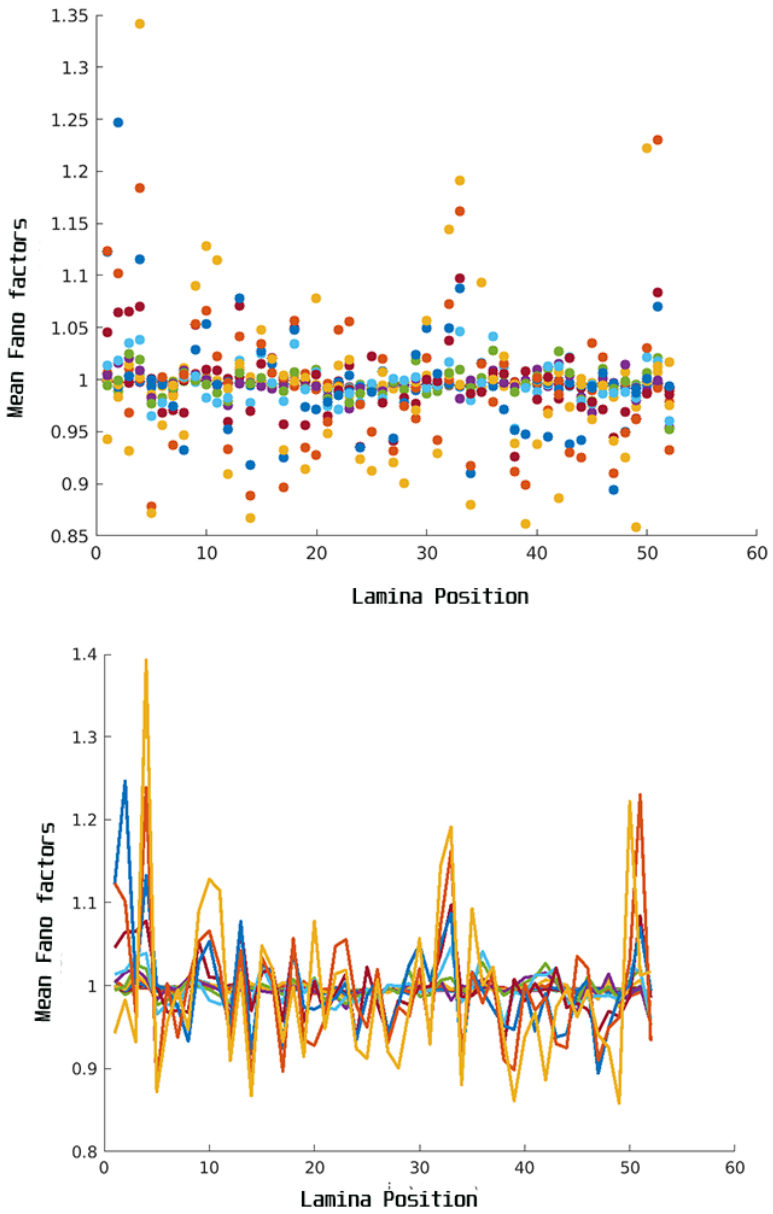

Scatter plot (TOP) and line plot (BOTTOM) of the mean fano factors from the Poisson spike trains that where artificially generated

The binsize dependence of FFs is thus explained away by mathematics, the observed depth dependence of FFs however; their increase and subsequent decrease with depth, is yet to be explained. Both rates and FFs seem to increase and decrease similarly with depth. A direct plot of average rates and FFs does not show much correlation (fig 7) as the depth may be a confounding variable that needs to be taken into account also.

Figure 7

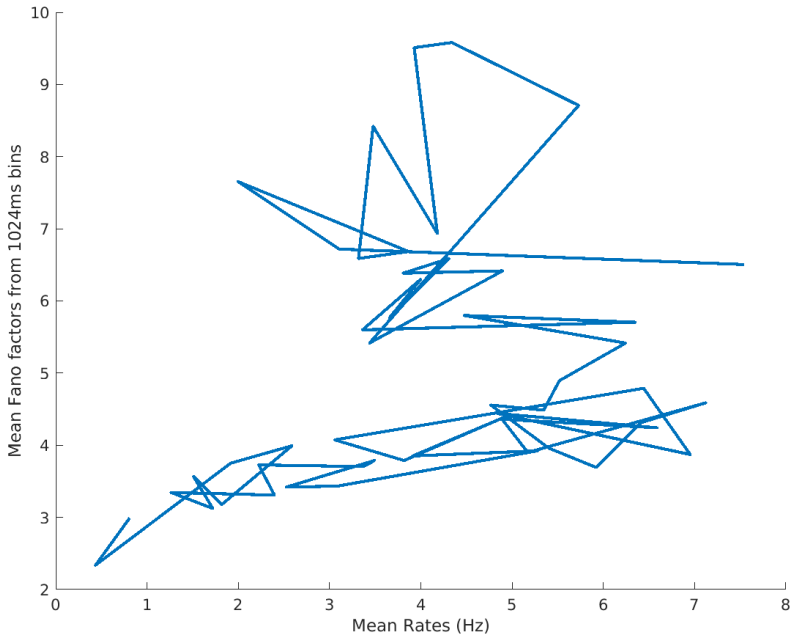

Thus the relationship between Fano factors and firing rates cannot be looked at in isolation. A multiple regression model was used to take the distance into account when probing the relationship between the firing rates and Fano factors ; with log of the mean firing rates and the depth (position/channels) as the two predictors of the continuous response (Fano factors) (fig. 8) shows the two predictors as accounting for 77% of the variation in Fano factors(i.e $R^2 = 0.7704, p < 0$). Fano factors from 1024ms binsizes where used in this plot

Figure 8

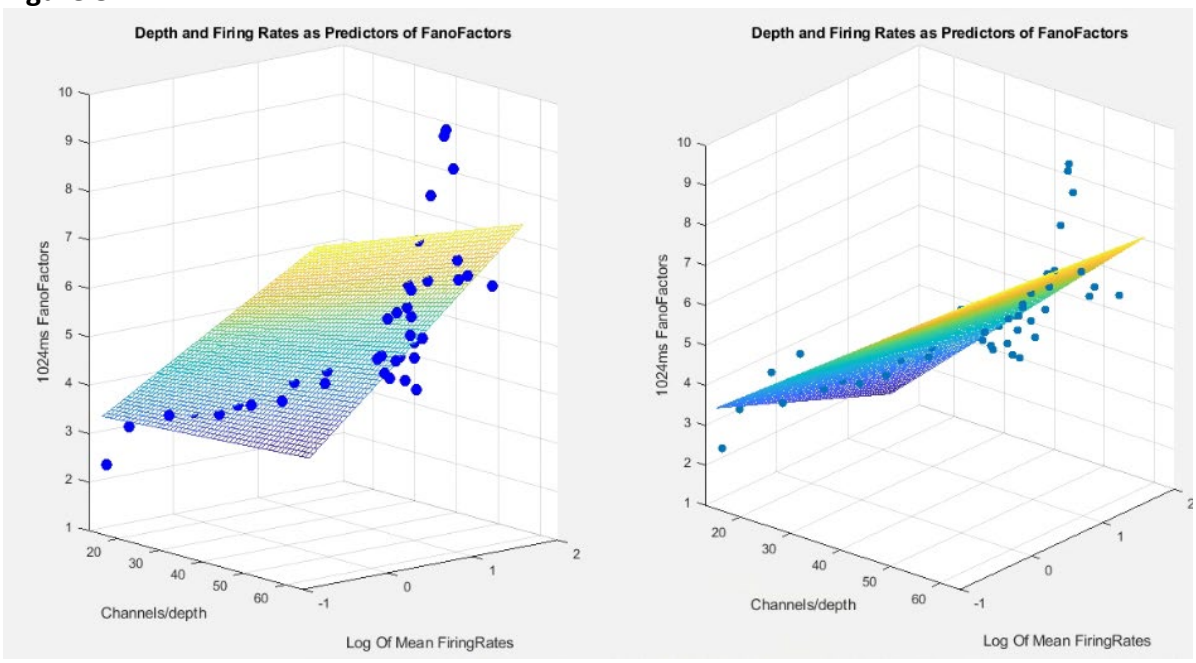

The R^2 value is observed to vary with change in binsizes used in generating the Fano factors. The line plot in figure 9 shows that it was highest with the smallest of binsizes (1ms and 2ms), bottoming out with Fano factors from 4ms bins, and afterwards increasing with an almost smooth curve, peaking at FFs from 512ms bins.

Figure 9

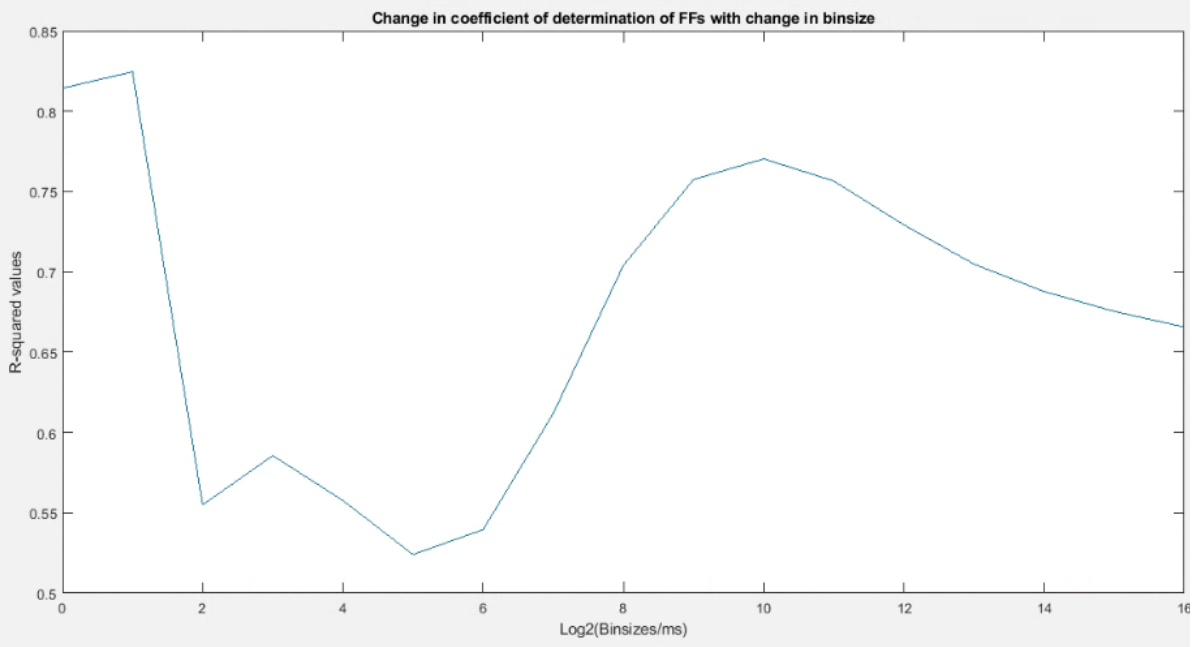

To determine the unique contributions of the individual predictors (Firing rates and position/distance) to the response (Fano factors) variance, the Proportional reduction in error (PRE) was worked out for each of the predictors. The PRE indicates the percentage of response variation generated by an individual predictor in a regression model that has one or more other predictors [9]. Figure 10 shows that firing rates have a larger influence on Fano factor variance than depth/position for the small binsizes. This dynamic flips around when progressively larger time bins (on a log 2 scale) are used.

Figure 10

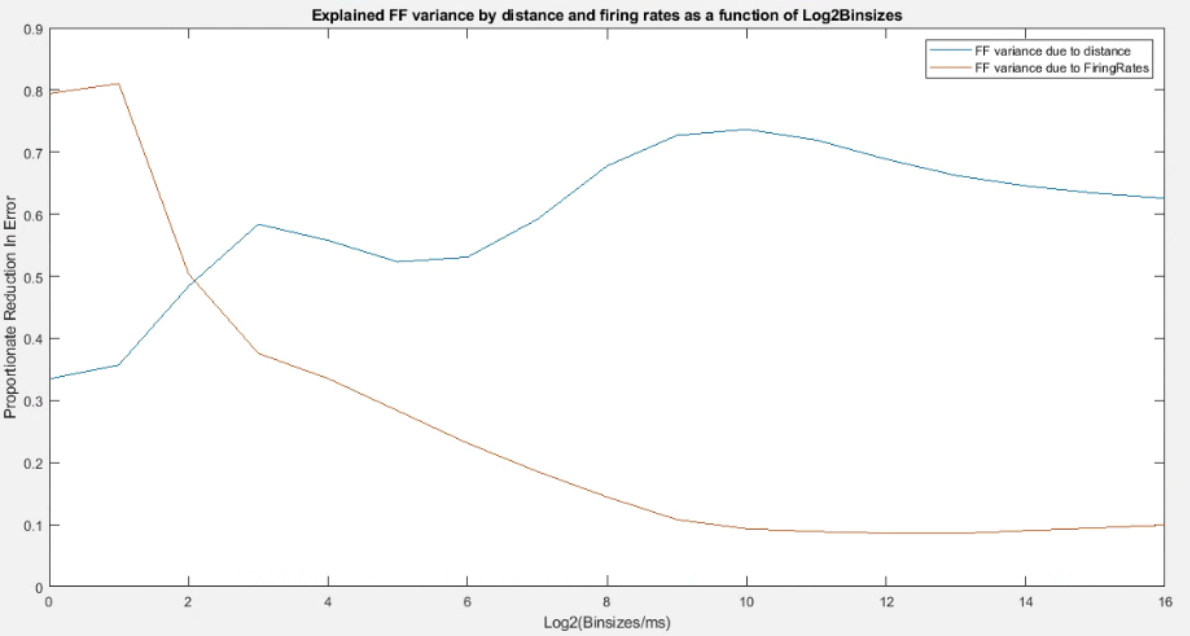

To further distil the relationship between individual predictors and the response, the partial correlation coefficient was worked out for each relationship using individual neuron variables as opposed to averaging units per recording channel; this way the variation in the values of the three variables in the neuronal population can be illustrated (Fig. 11). Partial coefficients come about by controlling the effect of a possible predictor whilst the predictor of interest is allowed to vary. This was carried out using Fano factors derived from the use of 17 different binsizes, giving rise to a binsize-course in the x-axis and the partial coefficients of correlation in the y-axis (blue lines). For comparison, "simple" correlation coefficients where also calculated where the effect of the other variable was not being controlled for (red lines). The coefficients for laminar position with FFs are mostly positive (max r=0.31, Fig. 11 B), whilst those for rates with FFs are mostly negative for the smaller binsizes (Fig. 11 A). In both cases, the relationship between the Fano factors and two variables under consideration is dependent on the size of the (spike-train) bin such that a high correlation exists between the correlation coefficients and the binsize; r=0.85 (Fig.11 A-Red), r=0.82 (Fig.11 A-Blue), r=0.93 (Fig.11 B-Red), r=0.83 (Fig.11 B-Blue).

Fig 11

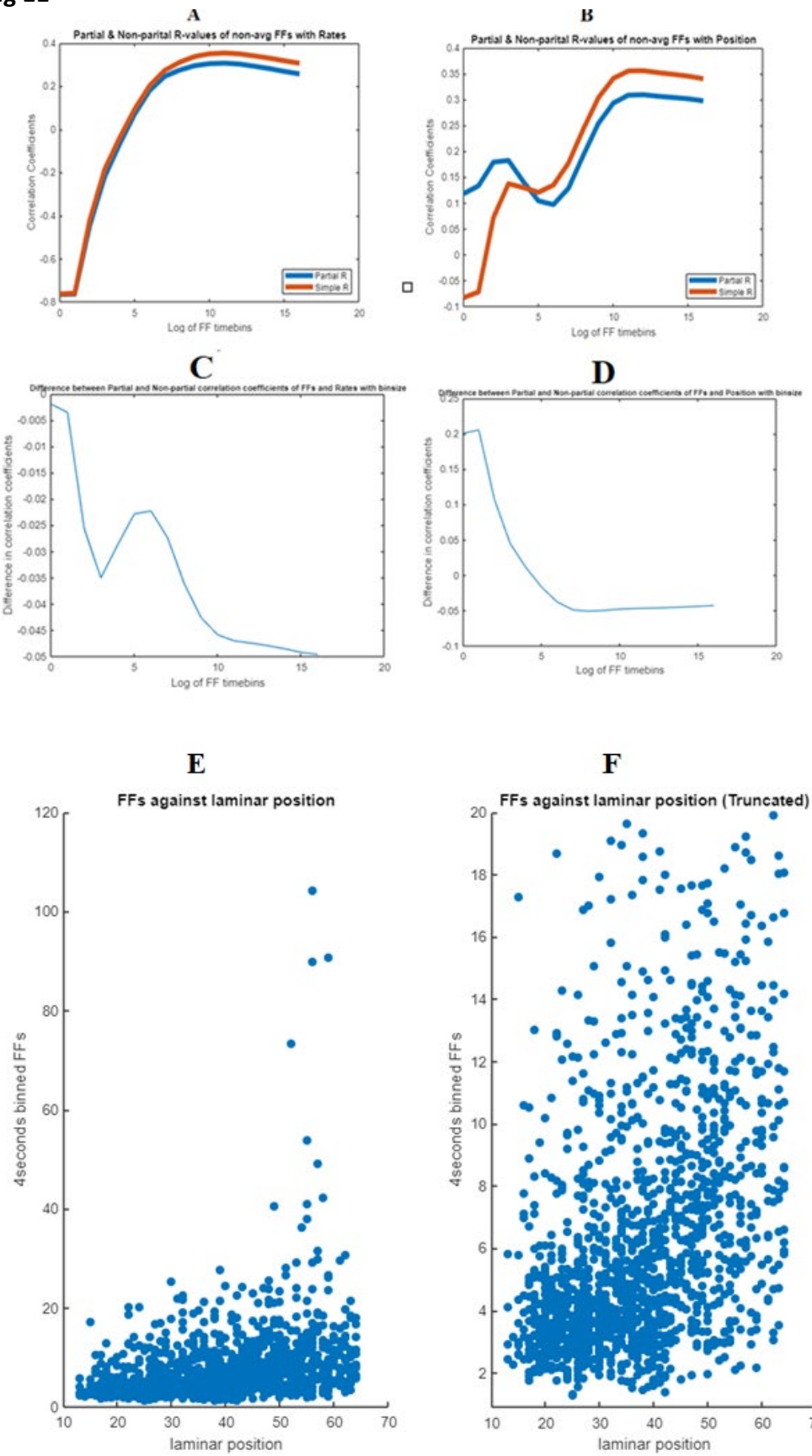
A
Partial & Non-parital R-values of non-avg FFs with Rates
Correlation Coefficients
Log of FF timebins
Partial R
Simple R
B
Partial & Non-parital R-values of non-avg FFs with Position
Correlation Coefficients
Log of FF timebins
Partial R
Simple R
C
Difference between Partial and Non-partial correlation coefficients of FFs and Rates with binsize
Difference in correlation coefficients
Log of FF timebins
D
Difference between Partial and Non-partial correlation coefficients of FFs and Position with binsize
Difference in correlation coefficients
Log of FF timebins
E
FFs against laminar position
4seconds binned FFs
laminar position
F
FFs against laminar position (Truncated)
4seconds binned FFs
laminar position

A:Figure shows the partial (blue line) and non-partial(red line) correlation coefficients for Fano factor of 17 different binsizes against laminar position
B: Shows the same coefficients as above but for Fano factors and rates
C-D: The figures show the difference between the partial and non-partial coefficients of correlation observed in graphs A and B
E-F: Graphs showing the plot of FFS against lamina position for FFs producing largest correlation;r=0.31. Figure F has truncated y-axis

The difference in the partial and non-partial correlation coefficients was worked out to determine the size of the effect of the third variable; if any exist at all. This was worked out for both FFs-Position and FFs-Rates for all 17 different FF time-bins. For Position and FFs, the graph (Figure 11-D) is initially slightly positive before becoming zero for the larger binsizes, suggesting that for the smaller binsizes, the third variable (Rates); naturally causes the FFs and Position to have a weaker correlation. Figure 12-C suggests that the third variable (position) causes a stronger correlation between the Rates and FFs such that controlling for its effects gives rise to smaller correlation coefficients, causing the negative difference seen.

Figure 13 shows how the different coefficients vary for a chosen binsize (1024ms). The "simple correlation" column shows correlation coefficients for when the third variable is not being controlled for. The "simple regression" column shows two R^2 values, one for Fano factors and rates, and the other for Fano factors and position. The multiple regression column on the other hand shows R^2 value for a multiple regression where both rates and position are used as predictors of Fano factors. All these measures were carried out for individual neurons (n=1471 with channel 1 excluded) as well as with averaged values per channel to probe variability at the individual level of a single neuron and to see how that compares with the emergent values from summed activity of neurons at each layer.

Figure 13

	Partial CorrCoef		Simple CorreCoef		Simple Regression (R^2)		Multiple Regression (R^2)	
	1471	AVG(52)	1471	AVG(52)	1471	AVG(52)	1471	AVG(52)
FFs & Rates	0.358	-0.297	0.369	0.358	0.136	0.111	0.228	0.760
FFs & Position	0.328	0.857	0.341	0.864	0.116	0.742		

The findings in this experiment thus strongly point out to depth/position as having a predictive effect on the FF value neurons possess, suggesting existence of a laminar organization that gives rise to the pattern of variance in spiketrains seen as the depth of the cortex is traversed

References

1. W. Gerstner and W. M. Kistler (2002)“Spiking Neuron Models. Single Neurons, Populations, Plas-ticity,” Cambridge University Press, Cambridge.
2. Z. Pawlas, L. B. Klebanov, M. Prokop and P. Lansky (2008) Parameters of spike trains observed in a short time window, Neural. Comput.,20, 1325–1343.
3. K. Rajdl and P. Lansky (2004) Fano Factor Estimation. Mathematical Biosciences and Engineering 11(1):105-123
4. R. Q. Quiroga and S. Panzeri, Principles of Neural Coding (Book) 343
5. B. Munn et tal (2020) Fractal spike dynamics and neuronal coupling in the primate visual system. The Journal Of Physiology. doi.org/10.1113/JP278935
6. M. Mancas () From Human Attention to Computational Attention: A Multidisciplinary Approach. Page 91
7. S. Koyama (2015) On the Spike Train Variability Characterized by Variance-to-Mean Power Relationship. Neural Computation.27(7): 1530-48. doi: 10.1162/NECO_a_00748
8. Hromádka T, et tal. (2008) Sparse representation of sounds in the unanesthetized auditory cortex. PLoS Biol 6:e16
9. F. J. Kviz (1981) Interpreting Proportional Reduction In Error Measures as Percentage of Variation Explained. Sociology Quarterly 22(3):413-420. Doi:10.1111/j.1533-8525.1981.tb00671.x
10. D. A. Rusakov et tal (2020) Noisy Synaptic Conductance: Bug or a Feature?. Trends in Neurosciences. 43(6): 363-372
11. Y. Senzai, A. F. Ruiz and G. Buzsaki (2019) Layer-Specific Physiological Features and Interlaminar Interactions in the Visual Cortex of the Mouse. Neuron. 101: 500-513. DOI:https://doi.org/10.1016/j.neuron.2018.12.009
12. M. Okun et tal (2019) Distinct Structure of Cortical Population Activity on Fast and Infraslow Timescales. Cerebral Cortex. 29(5):2196-2210. doi.org/10.1093/cercor/bhz023
13. A. S Charles et tal (2018) Dethroning the fano factor: A Flexible, Model-Based Approach to Partitioning Neural Variability. Neural Computation. 30(4):1012-1045. doi: 10.1162/neco_a_01062